Eur Biophys J 21, 137–145 (1992)

European Biophysics Journal

A theoretical study of glucosamine synthase

II. Combined quantum and molecular mechanics simulation of sulfhydryl attack on the carboxyamide group

A. Tempczyk [1], M. Tarnowska [1], A. Liwo [1], and E. Borowski [2]

[1] Department of Chemistry, University of Gdańsk, ul. Sobieskiego 18, PL-80-952 Gdańsk, Poland
[2] Department of Pharmaceutical Technology and Biochemistry, Technical University, PL-80-952 Gdańsk, Poland

Received November 19, 1991/Accepted in revised form November 27, 1991

Abstract. Continuing our theoretical studies of glucosamine synthase catalysis, we have carried out MNDO and ab initio calculations of the first stage of the reaction, which involves the attack of a cysteine thiol group from the enzyme active site on the side chain carboxyamide group of glutamine, producing ammonia and thioester. The reactants were modelled by methyl mercaptate and acetamide, respectively. For two considered mechanisms of the reaction the energy surfaces were evaluated. Mechanism I, proposed by Chmara et al. (1985) involves the nucleophilic attack of a deprotonated thiol group on the carbonyl carbon atom. Mechanism II, postulated in our previous work (Tempczyk et al. 1989), assumes the concerted binding of the mercaptate sulphur to the carbonyl carbon and the sulfhydryl hydrogen to the amide nitrogen with simultaneous breaking of the S—H bond. The energy surface of mechanism I shows no minimum on the approach of the mercaptide anion towards the carbonyl carbon, which is also consistent with ab initio calculations in a 4-31 G basis set. Therefore, mechanism I seems to be unlikely. The same analysis of mechanism II shows that it leads to the desired products: methyl thioacetate and ammonia. The presence of a sulfhydryl hydrogen causes apparent pyramidicity of the amido nitrogen and lengthening of the C—N bond in the transition state, making conditions for the release of the ammonia molecule. The MNDO calculated energy barrier of the reaction is 50.1 kcal/mol and the approximate 4-31 G ab initio barrier (at the MNDO geometries of the substrate complex and the transition state) is 63 kcal/mol. The biggest energy contribution to the barrier comes from the breaking of the S—H bond, which also causes a large charge separation in the transition state. The latter affect may result in the stabilisation of the transition state in a real enzymatic environment when compared to the gas phase, e.g. by the interaction of the reacting center with a pair of oppositely charged amino acid side chains such as lysinium and glutamate (aspartate), which are present in the enzyme studied. To estimate the magnitude of this effect, molecular mechanics calculations were carried out on the reaction center at the transition state in our proposed model of the enzymatic active site. The site was supplemented by ammonium and acetate ion, which were to mimic the lysinium and glutamate/aspartate side chains. A transition state stabilization energy of 20 kcal/mol was obtained and this lowers the energy barrier to about 30 kcal/mol. This value is within the thermal energy range of an average protein and indicates that our mechanism is a possible route of glucosamine synthase catalysis.

Key words: Glucosamine synthase – Enzymatic catalysis – Nucleophilic addition – MNDO and ab initio energy surfaces – Transition state stabilization

Introduction

Glucosamine-6-phosphate synthase (E.C.2.6.1.16) is a key enzyme in aminosugar metabolism in microorganisms. It has recently been shown that this enzyme can be a valuable target for selective antifungal agents (Andruszkiewicz et al. 1987; Andruszkiewicz et al. 1990; Milewski et al. 1988). The rational design of enzyme inhibitors requires the elucidation of its mechanism of action at the molecular level.

In the first paper of this series (Tempczyk et al. 1989), hereafter referred to as (I), we outlined our proposed mechanism of the action of glucosamine synthase and performed molecular mechanics calculations on two models of the enzyme active center, as well as on their complexes with the substrates – glutamine and fructose. One of these models of the active center assumes the *Escherichia coli* enzyme N-terminal sequence: Cys^1-Gly^2-Ile^3, while the second one involves the sequence Cys^{n-1}-Ala^n-Cys^{n+1} which is based on the experimental observa-

Offprint requests to: E. Borowski

tion that the enzyme subunits act in a correlated way. This, in turn, indicates the possibility of the proximity of two cysteine moieties in the amino acid sequence [the "covalent dimer"; see (I)].

As mentioned in (I), the main difference between the proposed mechanism of glucosamine synthase action and one postulated earlier by Chmara et al. (1985), as well as the related mechanism for the action of cysteine proteases (Drenth et al. 1976), is that instead of the removal of a proton from the sulfhydryl group of cysteine preceding the binding of the mercaptide anion to the carboxyamide group of glutamine a concerted binding of the thiol group is assumed, the sulphur attacking the carbonyl carbon and, simultaneously, the sulfhydryl hydrogen-nitrogen. This is facilitated by the similar dimensions of the C–N and S–H bonds. Our molecular mechanics calculations have shown that the configuration of the reacting fragments which is required for the reaction remains an energy minimum in the enzyme active center-substrate complex, even though we allowed for the full flexibility of the components.

The present study was aimed at answering two questions: *i*) Is our proposed reaction path energetically possible? and *ii*) Is it preferable to the binding of mercaptide anion after the prior removal of a proton? The second question is very important, as ab initio calculations (Dijkman et al. 1987) have shown that removal of the proton from the sulfhydryl group by the imidazole fragment, assumed as a model of the histidine side chain, leads to the proton-transfer state being less stable by only about 30 kcal/mol in vacuo and being more stable than the sulfhydryl ··· imidazole hydrogen bonded complex when the formate anion (bearing a charge of −1) is introduced to take the second imidazole proton (Umeyama and Nagakawa 1981). There is also much experimental evidence for the presence of a mercaptide anion in the active site of a related enzyme-papain (Polgar 1974; Lewis et al. 1976; Shinitzky and Goldman 1967).

The two mechanisms can be written schematically as follows:

Mechanism I (with deprotonation of sulfhydryl group):

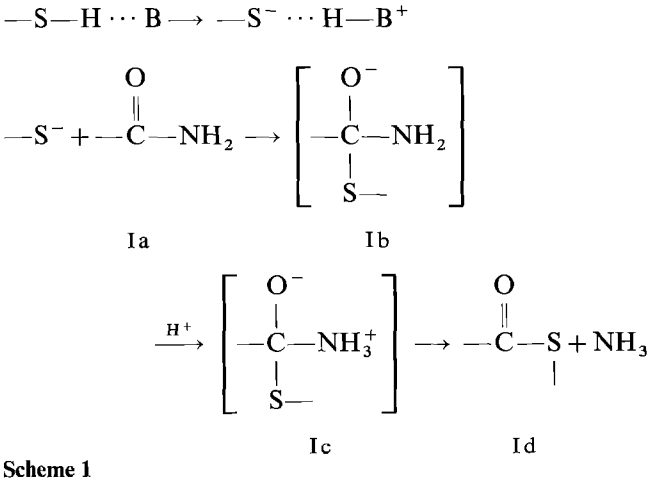

Ia Ib Ic Id

Scheme 1

Mechanism II (concerted binding):

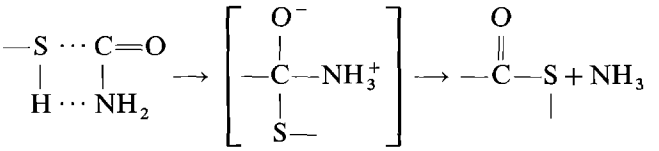

IIa IIb IIc

Scheme 2

The forms in square brackets can be either intermediates (energy minima) or transition states (saddle points on the energy surface). The ammonia molecule liberated in the final stage binds to the hemiacetal carbon of fructose, initiating the process of amination of this sugar, thus leading to the formation of glucosamine.

In the present study, using the semi-empirical quantum mechanical MNDO method (Dewar and Thiel 1977), we have evaluated the energy surfaces corresponding to the two mechanisms given. As the results of the semi-empirical calculations are not fully reliable, especially when changes in the bond net occur, for some characteristic points we have performed SCF ab initio calculations in the 4-31 G basis set, which has been shown to lead to reliable results when the sulphur atom is involved (Howard and Kollman 1988; Dijkman et al. 1987; Umeyama and Nagakawa 1981). Finally, molecular mechanics calculations have been performed to estimate the stabilization of the intermediate by the environment.

Methods

All the calculations were carried out on a PC AT computer equipped with an 8087 arithmetic coprocessor.

It is evident that such changes as the breaking of old and forming of new bonds can be described only at the quantum mechanics level. However, this restricts the simulation to the very center of the reaction, as the computation time and core requirements increase with the fourth power of the number of orbitals involved. We have therefore taken acetamide as the model of the glutamate side chain and methyl mercaptate as the model for protonated and deprotonated cysteine.

As mentioned, the energy surfaces were constructed using the MNDO method. Calculations were carried out with the use of a PC-adapted version of the MNDO program of Dewar and Thiel (1977), without d-functions on sulphur. Estimated partial derivatives were used in geometry opimization. In the case of mechanism I the energy was evaluated as a function of the C ··· S distance (x), while for mechanism II it was evaluated as a function of both the C ··· S (x) and N ··· H (y) distances. Except for the valence geometry of methyl groups, which was taken as standard (1.1 Å and 109.47° for the C–H bond length and C–C–H and H–C–H angles, respectively) all the remaining degrees of freedom were energy-optimized at each point. The choice of variables for both mechanisms is shown in Fig. 1.

The energy was evaluated on a one- and two-dimensional grid of points for mechanism I and II, respectively.

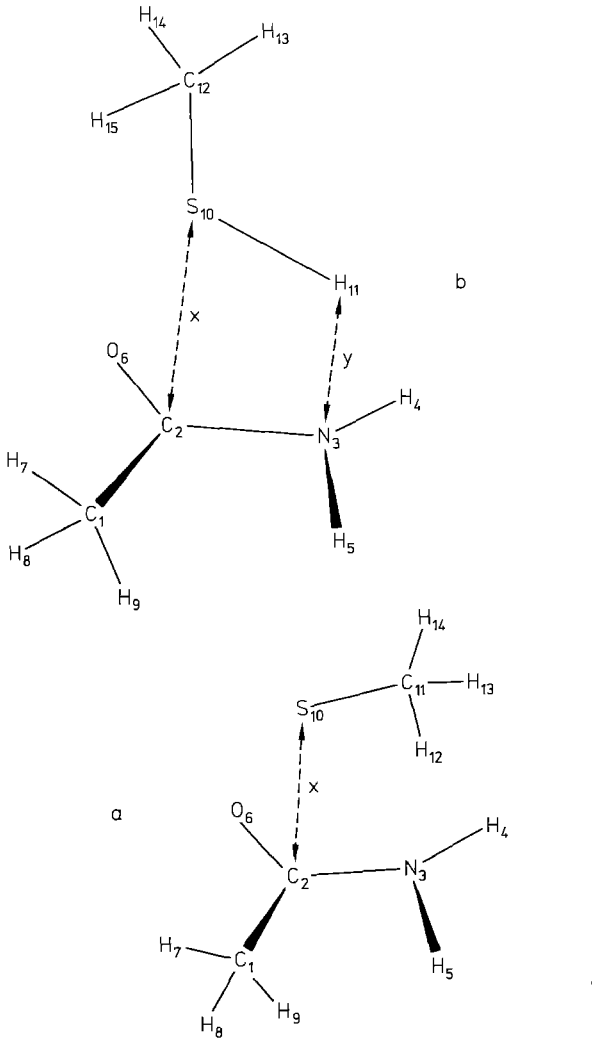

Fig. 1. The choice of variables and atom numbering system for mechanism I (**a**) and II (**b**)

The increment in the variables was usually 0.2 Å. For mechanism II in regions of rapid energy changes, as well as in the neighbourhood of the transition point, step lengths of 0.05 Å were taken to increase accuracy.

SCF ab initio calculations were carried out in the 4-31 G basis set with the use of the program MICROMOL (Colwell et al. 1985) which is a PC-adapted fragment of the CADPAC package (Amos 1984).

Molecular mechanics calculations were carried out with the use of the AMBER force field (Weiner et al. 1984) which implies the relaxation of all degrees of freedom. The software used was Allinger's MM2 (Allinger and Yuh 1977) which we modified heavily in order that it can handle the AMBER force field (Liwo et al. 1988). The changes of the transition state on the methyl mercaptate-acetamide energy surface used in these calculations were estimated based on the electrostatic potential computed from the CNDO/2D wave function, as described elsewhere (Liwo et al. 1988). In an earlier paper (Liwo et al. 1988) we proved that they are sufficiently compatible with the 6-31 G ab initio wave function electrostatic potential used in the AMBER force field (Weiner et al. 1984).

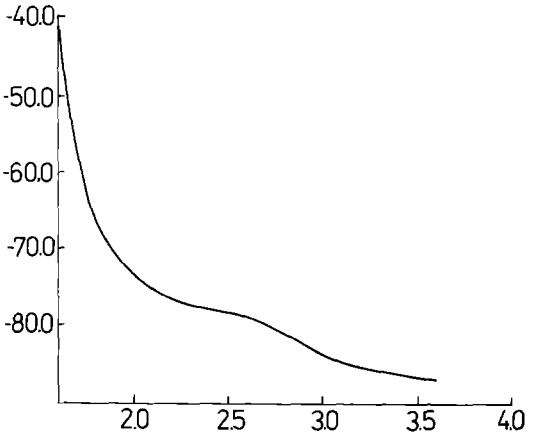

Fig. 2. MNDO heat of formation curve for mechanism I (values in kcal/mol)

Results and discussion

The MNDO energy surfaces

The MNDO energy curve corresponding to mechanism I is shown in Fig. 2, while the energy map of system II is shown in Fig. 3. In Fig. 3 we also indicate the reaction path (the gradient path of the minimal energy integral).

As shown, no energy minimum, but only a turning point, appears at $x \cong 2.4$ Å on the energy curve of mechanism I. This means that the mercaptide anion cannot bind to the amide bond. This result conforms with earlier ab initio calculations of Howard and Kollman (1988) which have shown that the hydrosulphide, as opposed to the hydroxide anion, cannot form a tetrahedral adduct with formamide, even if a stabilizing solvation effect is taken into account. Our result is in clear contradiction with the mechanism of Chmara et al. (1985), as the latter assumes that the ionization of the sulfhydryl is necessary in order to enable the binding to the carbonyl carbon.

Because using semi-empirical methods only cannot be a strong enough basis for such an important conclusion, we have calculated some points from the assumed binding region of the energy curve using the ab initio method with the 4-31 G basis set. Owing to the storage limitations of MICROMOL, we had to substitute both methyl groups by hydrogens with bond lengths of 1.34 Å for the S–H and 1.07 Å for the C–H bond, respectively. The rest of the geometry was taken from the appropriate points of the MNDO energy curve. The results, compared with the MNDO energies, are summarized in Table 1. As shown, ab initio also gives no energy minimum in the region investigated and results in a strong repulsion when the C ··· S distance is less than 2.0 Å.

The conclusion that there is no binding in the case of mechanism I is also justified by the fact that there is little change in the valence geometry of acetamide on approaching the $S-CH_3^-$ anion, only the amide nitrogen becoming a little pyramidal owing to strong electrostatic interactions of the amide hydrogens with the negatively charged sulphur atom (see Fig. 4 for the drawing of the geometry of the turning point and Table 2 for comparing

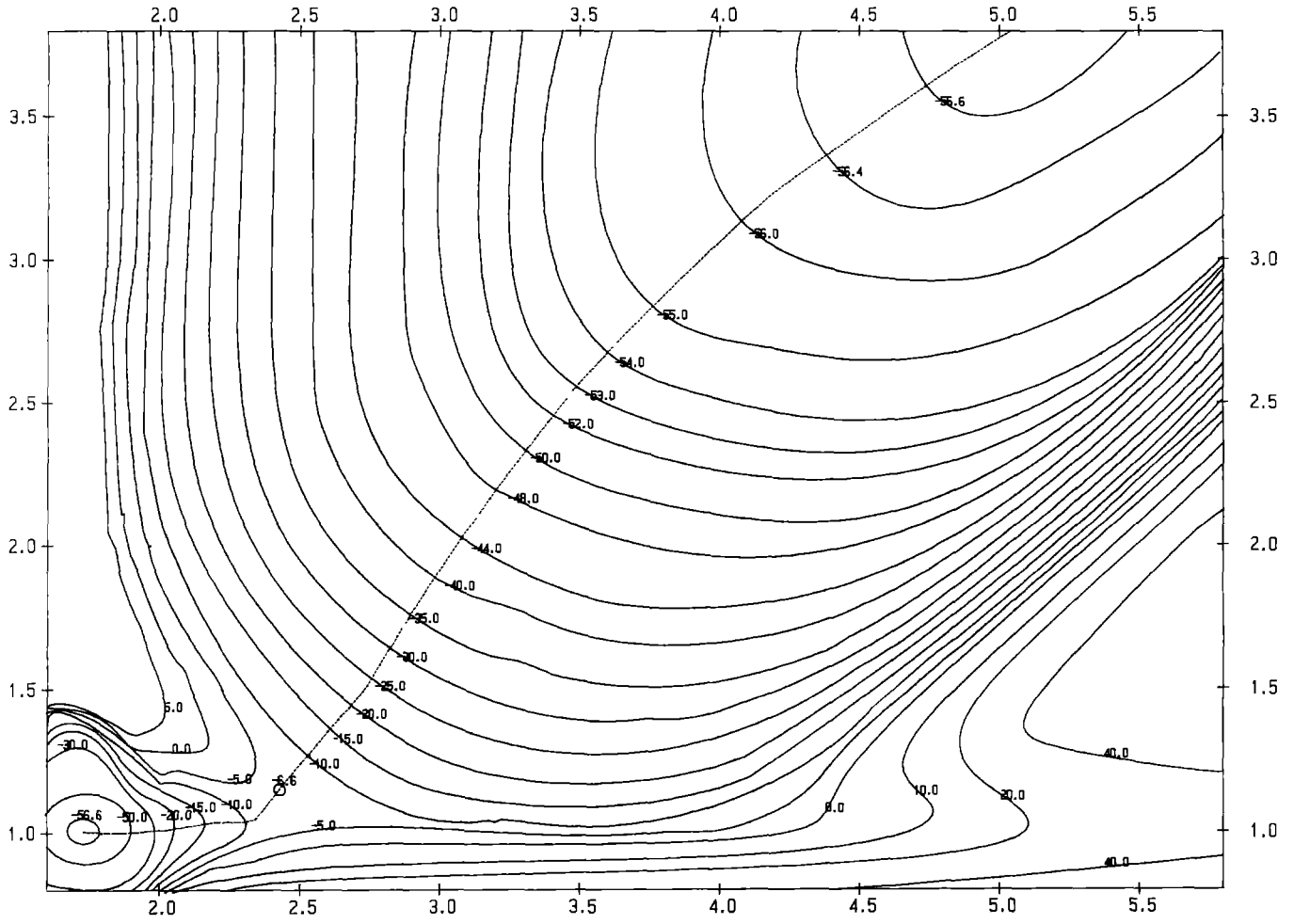

Fig. 3. MNDO heat of formation energy map for mechanism II: *abscissa* – x (values in Å); *ordinates* – y (values in Å); *solid lines* – equi-energetic curves (values in kcal/mol); *dotted line* – the reaction path; the saddle point being encircled

Table 1. Comparison of the MNDO and ab initio energies at some points of the reaction curve of mechanism I

	Total energy [eV]		ΔE [kcal/mol]*	
x [Å]	MNDO	ab initio	MNDO	ab initio
2.4	−1266.72	−15421.50	0.0	0.0
2.2	−1266.64	−15421.10	1.8	9.2
2.0	−1266.55	−15420.60	3.9	20.8
1.8	−1266.26	−15420.22	10.6	29.5

* $\Delta E = E(x) - E(x = 2.4\,\text{Å})$

Table 2. Comparison of the valence geometry of acetamide at the turning point of the energy curve of mechanism I with that of free acetamide (see Fig. 1 for atom numbering and Fig. 4 for structure)

Bond/angle	Value [Å/deg]	
	Free*	Turning point
C(2)–N(3)	1.39	1.45
C(2)–O(6)	1.23	1.24
N(3)–C(2)–O(6)	118.4	123.2
N(3)–C(2)–C(1)	117.7	117.4
C(2)–N(3)–H(4)	122.1	111.8
H(4)–N(3)–H(5)	115.4	105.7

* MNDO optimal values

the geometry of free acetamide and its geometry at the turning point). Moreover, according to scheme I, the oxygen atom should bear a formal charge of −1 in intermediate I b, if the C–S bond is to be formed. The analysis of the MNDO and 4-31 G populations shows that for all the points considered the negative charge is located on the sulphur atom and no charge transfer to acetamide takes place.

The inspection of the energy surface corresponding to mechanism II reveals that there are two energy minima, one of them corresponding to noncovalent mercaptate ··· acetamide complex, the second one to the products. The two minima are linked by a reaction path with a clear transition point at $x = 2.42$ Å, $y = 1.15$ Å. Additionally, the geometries of the substrate and product complexes were energy optimized with the relaxation of all the degrees of freedom. The three structures discussed are displayed in Fig. 5 a–c and the geometrical parameters are shown in Table 3.

Another lower energy region is observed for $x > 5.0$ Å and $y = 1.0$ Å at which point an energy minimum must also be located. This minimum corresponds to the proton transfer state from the sulfhydryl group to the acetamide nitrogen.

As shown, the products are methyl thioacetate and ammonia, just as indicated in Scheme II. Structure II b is

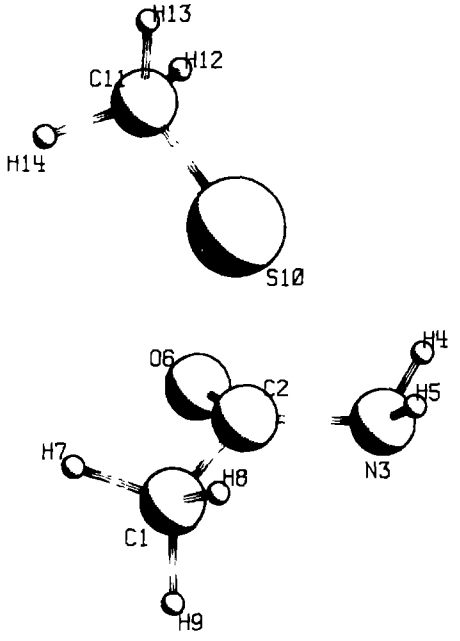

Fig. 4. $CH_3S^- \cdots CH_3CONH_2$ geometry at turning point (Fig. 2)

Table 3. Geometric parameters of the substrates, transition point, and products of the reaction occurring according to mechanism II (see Fig. 1 b for atom numbering and Figs. 5 a–c for structures)

	Substrates	Transition state	Products
Bond lengths and other interatomic distances [Å/deg]			
C(2)–N(3)	1.42	1.52	4.53
C(2)–O(6)	1.23	1.22	1.22
C(2)–S(10)	4.21	2.45	1.73
N(3)–H(4)	1.00	1.00	1.01
N(3)–H(5)	1.00	1.00	1.01
N(3)–H(11)	3.51	1.15	1.01
S(10)–H(11)	1.31	1.66	5.14
Bond and other planar angles [deg]			
C(1)–C(2)–N(3)	117.2	117.5	79.6
C(1)–C(2)–O(6)	124.4	126.9	125.5
C(1)–C(2)–S(10)	79.2	94.5	111.6
C(2)–N(3)–H(4)	116.3	113.5	79.6
C(2)–N(3)–H(5)	115.8	112.8	110.3
C(2)–N(3)–H(11)	96.9	100.6	106.0
Dihedral angles [deg]			
C(1)–C(2)–N(3)–H(4)	195.3	208.9	225.1
C(1)–N(3)–C(2)–O(6)	175.8	194.1	275.5
C(1)–N(3)–C(2)–S(10)	79.2	75.5	96.0
C(2)–H(4)–N(3)–H(5)	131.1	121.1	
S(10)–C(2)–N(3)–H(11)	7.6	3.1	

a transition point in the energy surface and, as shown in Fig. 5 b, the C(2) carbon is in a distorted trigonal pyramidal, rather than tetrahedral, surrounding.

The heats of formation corresponding to the substrate complex, transition state, and product complex are −56.7, −6.6, and −57.4 kcal/mol, respectively. There is thus almost no energy difference between the substrates and products, as far as the *isolated* reacting center is concerned, and the energy barrier of the reaction is 50.1 kcal/

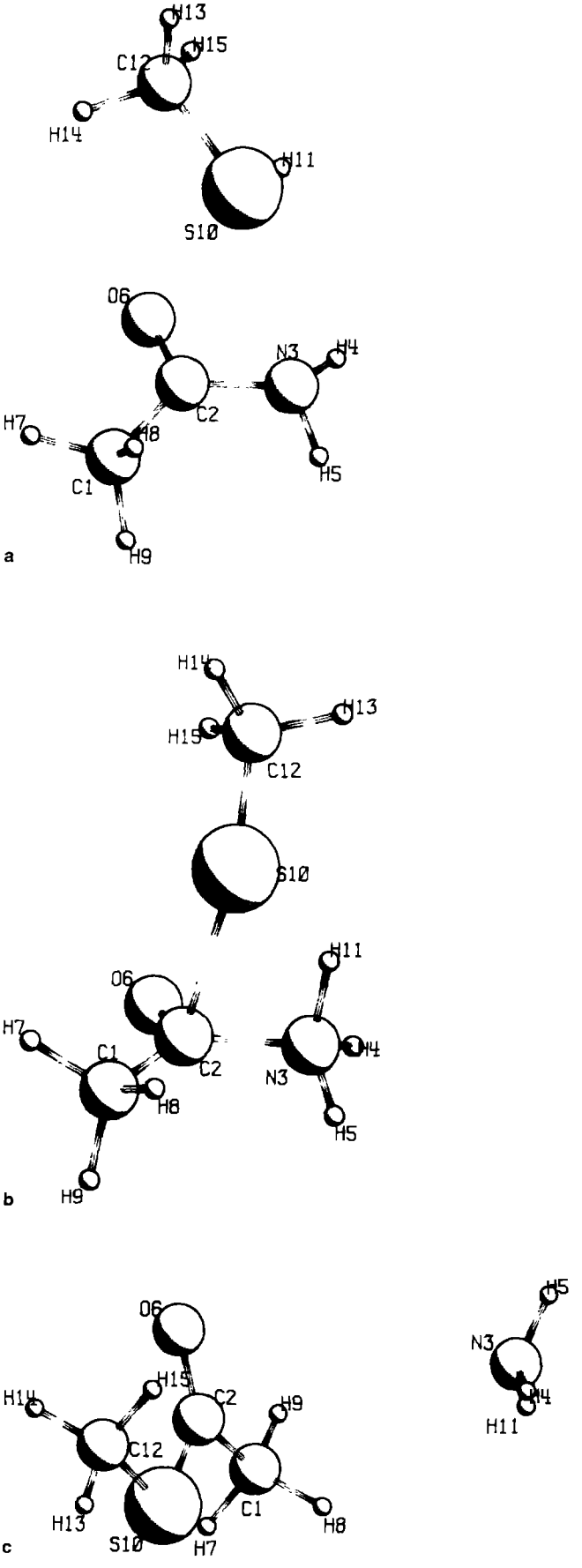

Fig. 5 a–c. The geometry of the critical point in the energy map of mechanism II: **a** substrate ($CH_3SH \cdots CH_3CONH_2$) complex: **b** transition state; **c** product ($CH_3COSCH_3 \cdots NH_3$) complex

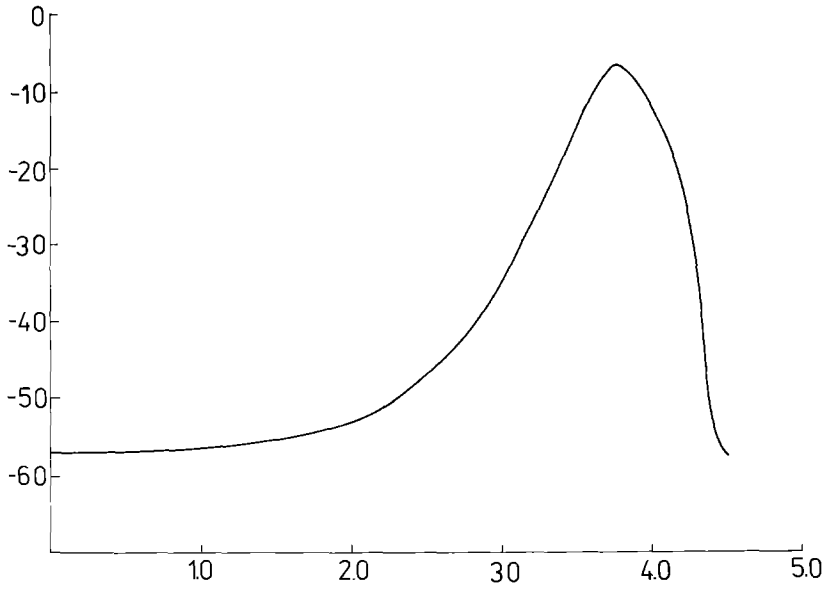

Fig. 6. Energy variation along the reaction path for mechanism II (Fig. 3) (values in kcal/mol)

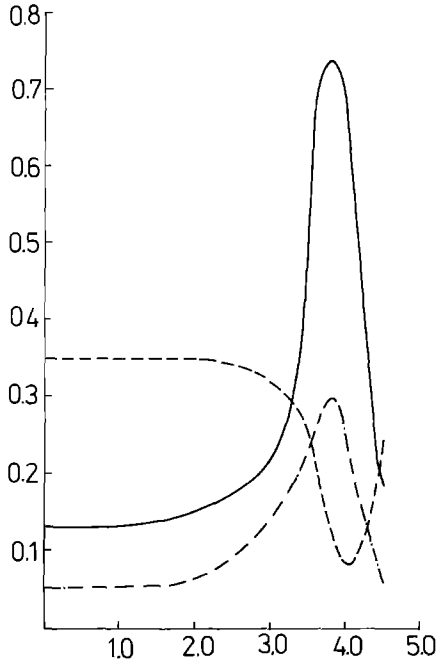

Fig. 7. Charge variation along the reaction path for mechanism II· *solid line* – the absolute value of S(10) charge; *centered line* – H(11) charge; *broken line* – the absolute value of N(3) charge. Electron charge units are used. The atoms S(10) and N(3) are always charged negatively, while H(11) is charged positively

mol. Energy variation along the reaction path is shown in Fig. 6.

Analysing the changes of the charge distribution and valence geometry we can describe the nature of the processes occurring during the reaction investigated. The MNDO net charge of the atoms subject to the greatest changes are plotted against the reaction coordinate in Fig. 7. As shown, there is a great charge separation on the reaction, the maximum being just in the transition state. The negative charge is transferred to S(10), while the positive charge is transferred mainly to H(11), C(2), N(3), and O(6), the total charge separation being about 0.5 e. The "formal" description, in which the total negative charge is assigned to the oxygen atom and the total positive to the nitrogen atom, as shown in Scheme IIb and assumed also in the mechanism of the action of the cysteine proteases (Drenth et al. 1976), therefore has little physical reality.

The localization of the negative charge on sulphur shows that it is only very weakly bonded to carbon in the transition state. In fact, the corresponding Wiberg index is only 0.14. On the other hand, we can say that the S–H bond has already been broken and a new N–H bond has begun to form, as the S ··· H distance is about 1.66 Å, compared with the 1.34 Å bonding distance, while the N ··· H distance is 1.15 Å, compared with 1.00 Å bonding distance. The Wiberg indices of the S(10)–H(11) and N(3)–H(11) bonds are almost equal: 0.43 and 0.49, respectively.

Interesting observations can also be made when analysing the change of the C(2) ··· N(3) distance along the reaction path (Fig. 8). As shown, a rapid change of this distance, which corresponds to the breaking of the C(2)–N(3) bond, occurs just after the transition point. Also at the transition point this bond is lengthened to as far as 1.52 Å, compared with the 1.43 Å corresponding to a single C–N bond. We can thus say that in the transition state this bond has just begun to break. In fact, the corresponding Wiberg index is 0.86. It should also be noted that the C(2)–O(6) bond remains double, its Wiberg index being 1.85.

All these facts indicate that rather than consider the covalent structure IIb, we should describe the transition state as in the case of the cycloaddition reactions, as shown in Scheme III:

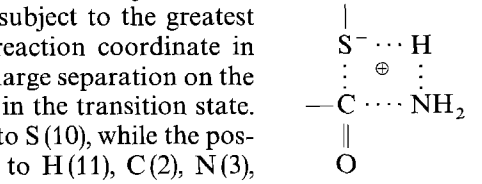

Scheme 3

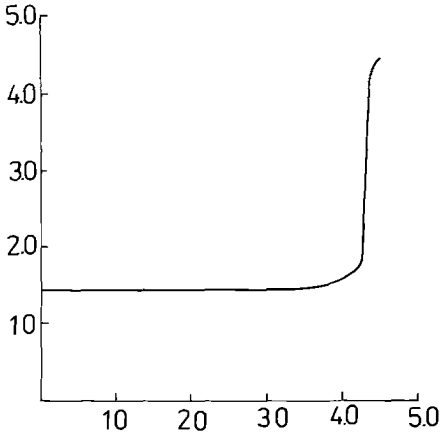

Fig. 8. C (2)–N(3) distance variation along the reaction path (values in Å)

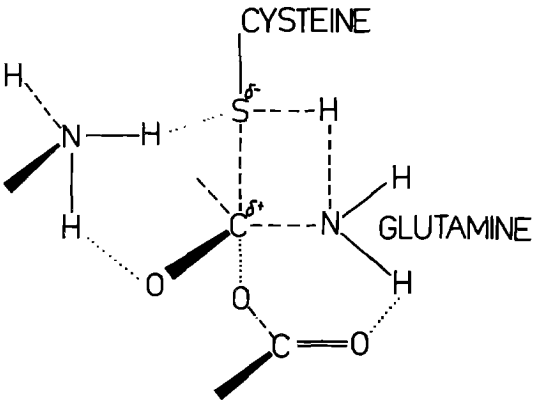

Fig. 9. Schematic representation of transition state stabilization

Possible stabilization of the transition state

The reaction barrier of about 50 kcal/mol seems to be high, but is reasonable in view of the fact that the transition point, to a rough approximation, it corresponds to the breaking of the S–H bond. To make sure that the height of the barrier is not an artefact of the MNDO method, we have calculated the substrate complex, transition point, and product complex using the SCF ab initio method with the 4-31 G basis set. As for mechanism I the methyl groups were substituted by hydrogens and the MNDO geometries were used. The corresponding energies are −567.3106, −567.2059, and −567.2848 a.u., respectively, indicating an energy barrier of 63 kcal/mol, in good agreement with MNDO results.

Keeping in mind that large charge separation occurs in the transition state, we can expect its significant stabilization in the polar protein environment which constitutes the enzymatic hole. Assuming a charge separation of 0.5 e, assuming that the solvation surface of each charge is a hemisphere of radius of 3 Å (the van der Waals sphere), and making use of the Born formula (Born 1920), we can estimate the upper bound of the stabilization energy to be about 28 kcal/mol (assuming that the dielectric constant is so high that its inverse is small compared with unity). If we allow spherical solvation surfaces of the same radius, the stabilization energy is increased by a factor of two. In reality, in a highly polar environment, we can thus expect a stabilization energy from about 28 to about 56 kcal/mol. This lowers the barrier to 22.3 kcal/mol at most and in optimal situations removes it all together.

Taking into account the nature of the transition state, we can try to explain its stabilization at the microscopic level. In fact, owing to large charge separation, it is very likely that this stabilization is a result of the presence of a counter ion pair in the enzymatic hole, for example the lysinium and glutamate (aspartate) side chains. The first of these will form hydrogen bond(s) with S(10), and the second one with the ammonium group being formed, as shown in Fig. 9. Both amino acids, as well as other amino acids with charged functions have been found in the *Escherichia coli* glucosamine snythase (Badet et al. 1987). Prelimimary estimation of the stabilization energy can be

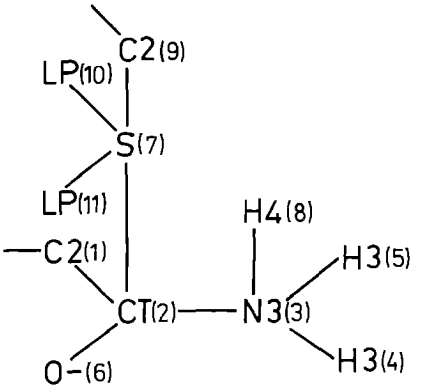

Fig. 10. Molecular mechanics atom types and atom numbering of the reacting center in the transition state

made taking a four-point charge model, in which the transition state is represented by two opposite charges of 0.5 e separated by a distance of about 2.5 Å, while the lysinium and glutamate group are represented by opposite unity charges. Assuming interaction spheres of 3 Å, we obtain a stabilization energy from 25.6 to 50.3 kcal/mol, depending on orientation.

To make a more extended model of the stabilized transition state, we incorporated it into our proposed model of the active center of glucosamine synthase which contains the *Cys-Ala-Cys* sequence and evaluated the geometry and stabilization energy using molecular mechanics. The reacting center was fixed at the MNDO geometry. The lysinium and glutamate side chains were simulated by ammonium and acetate, respectively, the charges being taken from Weiner et al. (1984). As indicated in the methods section, the charges of the reacting fragment were computed from its molecular electrostatic potential. They are summarized in Table 4, the atom numbering system and molecular mechanics atom types of the reacting center being shown in Fig. 10.

It is interesting that the charges fitted to molecular electrostatic potential show that the greatest polarization occurs along the C(1)–S(10) bond and that the total charge of the NH_3 fragment is almost zero, thus "prepar-

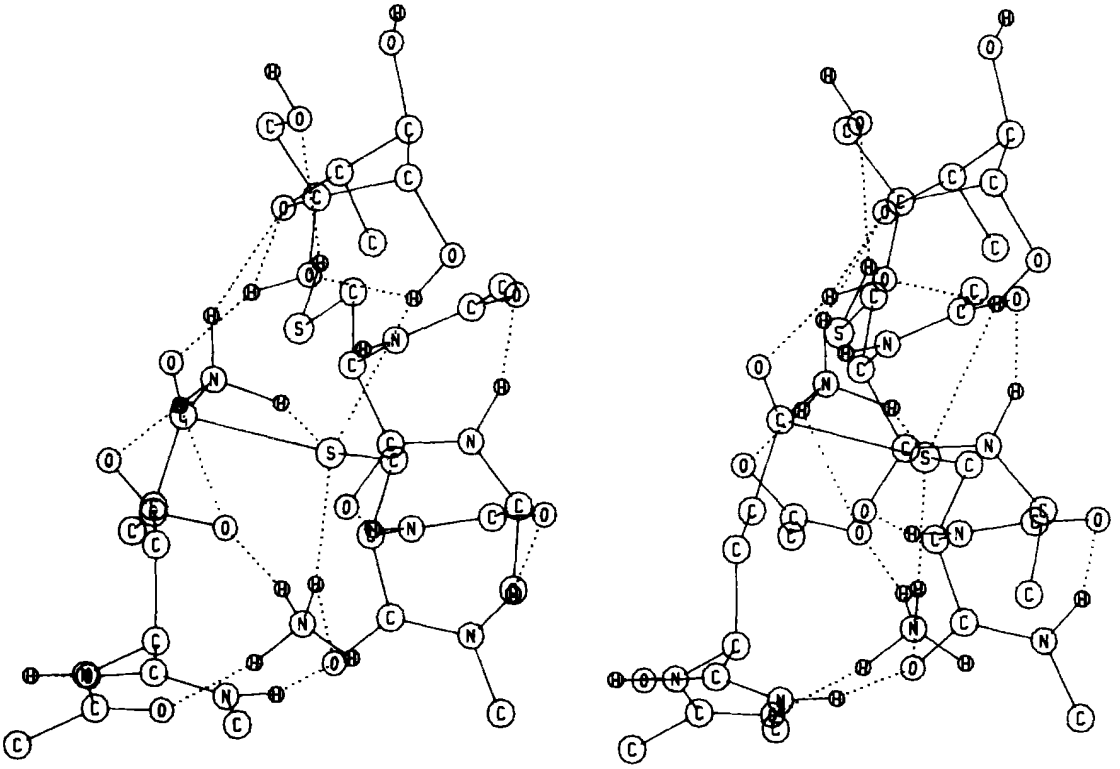

Fig. 11. Stereoview of the energy optimized structure of the transition state in the proposed active site model

Table 4. CNDO/2 potential charges used in molecular mechanics calculations

Atom*	Charge [e]
C2(1)	−0.057
CT(2)	1.046
N3(3)	−0.789
H3(4)	0.341
H3(5)	0.341
O^-(6)	−0.612
S (7)	0.438
H4(8)	0.289
C2(9)	−0.044
LP(10)	−0.450
LP(11)	−0.450

* Molecular mechanics united-atom types indicated; for change of numeration, see Fig. 10

ing" the system to lose ammonia. Anyway, it is confirmed that a charge separation of about 0.5 e occurs.

The energy optimized geometry of the transition state in the enzymatic hole is shown in Fig. 11. As shown, the ammonium and acetate ions work as expected. Because we have not imposed constraints on these ions, they form a pair which interacts with the transition state.

To evaluate the stabilization energy, after the geometry optimization we performed separate calculations of the steric energy of the system in two states: with the charges as in the transition state and after depolarization. The depolarization was achieved by adding −0.5 e to the charge of C(2), and +0.4 e and +0.1 e, to S(11) and O(6), respectively. Moreover, as the internal charge separation energy of the reacting center is included in its quantum mechanical energy, we calculated and then subtracted from the total energy of either polarization state the steric energy of the lone center. In all the calculations, except for geometry optimization, we used a dielectric constant $\varepsilon = 1.0$. If an ordinary distance-dependent dielectric constant were used, we would lose a part of stabilization energy, as it would be included in the interaction with the bulk of the environment, not present in the steric energy.

We have obtained a stabilization energy of 20 kcal/mol. In view of the fact that such an arrangement of the stabilizing ions, in which they form an ion pair, is not the optimal one from the point of view of the stabilization of the transition state, as there is small difference in the distance of either ion from the positively and negatively charged part of the latter, it can be regarded as a lower bound. Anyway, even this lowers the barrier significantly and makes it possible for the reaction to take place owing to thermal motion.

Conclusions

The results presented have shown that of the two mechanisms considered only the concerted attack of the hydrosulphide on the carboxyamide group can be justified on the basis of theoretical calculations. The prior deprotonation of sulfhydryl group clearly prohibits any binding of the sulphur atom to the carbonyl carbon.

The pyramidal (rather than tetrahedral) transition state obtained is characterized by a large separation, the negative charge being located on sulphur. This ensures that the obtained energy barrier, 50.1 kcal/mol, can be

lowered significantly in a polar environment. Moreover, this can shed light on the structure of the active center of glucosamine synthase which is still unknown, as it is very likely that the transition state is stabilized by a pair of oppositely charged amino acid side chains. This is justified by the fact that amino acids residues are present in the active center of papain (Drenth et al. 1976).

We have also shown that the ammonia molecule (in statu nascendi) which is needed for the amination of the sugar is clearly produced in the reaction center as a result of the first stage of the catalytic process (it is well known that owing to the lack of ammonia binding sites in glucosamine-6-phosphate synthase ammonia cannot be utilized when supplied from the environment). This is one more argument in favour of our proposed models of the enzyme-substrate complexes, as they assume fructose in the immediate neighbourhood of the γ-amino group of glutamine.

The results obtained in this study allow us also to postulate an alternative mechanism for the nucleophilic sulfhydryl attack on the carboxyamide moiety of glutamine. As mentioned, the main origin of the large energy barrier in our mechanism comes from the breaking of the cysteine S–H bond. The presence of an additional agent, say the imidazole moiety of histidine, able to take the sulfhydryl proton from cysteine would therefore be desirable. Because the ionized sulfhydryl group alone cannot attack the carbonyl carbon, either the sulfhydryl proton taken by histidine or, more probably due to steric conditions, a proton from another source (possibly another protonated histidine) must be supplied at the same time to bind to the carboxyamide nitrogen of glutamine, this enabling the formation of the C–S bond with simultaneous loss of the ammonia molecule, as for the mechanism studied in this work. The scheme of this alternative mechanism is shown in Fig. 12.

It can easily be concluded that such a mechanism links our earlier idea of the necessity of sulphur deprotonation prior to attack (Chmara et al. 1985) with our, as well as other authors' (Howard and Kollman 1988) results indicating that the formation of a tetrahedral intermediate is impossible with ionized sulphur. It conforms also with the experimental evidence for the presence of an ionized cysteine side chain in cysteine proteases, e.g. papain (Polgar 1974; Lewis et al. 1976; Shitnitzky and Goldman 1967). Further theoretical studies are, however, required in order to support it. These studies are now being carried out in our laboratories.

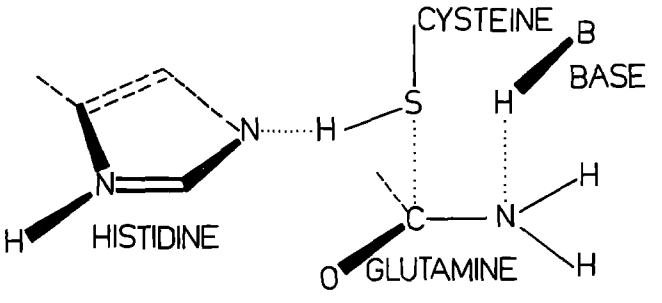

Fig. 12. Schematic representation of the alternative mechanism of the first stage of catalysis discussed in the text

Acknowledgements. The authors acknowledge the financial support of this study by the Project RP.II-10 of the Ministry of National Education.

References

Allinger NJ, Yuh YH (1977) QCPE, program No. 395

Allison EH, Kollman PA (1988) OH^- versus SH^- nucleophilic attack on amides: Dramatically different gas-phase and solvation energetics. J Am Chem Soc 110:7195–7200

Amos RD (1984) CADPAC, Cambridge analytical derivatives package, Publication CCPI/84/4, Daresbury, SERC, 1984

Andruszkiewicz R, Chmara H, Milewski S, Borowski E (1987) Synthesis and biological properties of N^3-(4-methoxyfumaroyl)-L-2,3-diaminopropanoic acid dipeptides, a novel group of antimicrobial agents. J Med Chem 30:1715–1719

Andruszkiewicz R, Milewski S, Zieniawa T, Borowski E (1990) Anticandidal properties of N^3-(4-methoxyfumaroyl)-L-2,3-diaminopropanoic acid oligopeptides. J Med Chem 33:132–135

Badet B, Vermoote P, Haumaut P, Lederer F, Le Goffic F (1987) Glucosamine synthetase from *Escherichia coli*: Purification, properties, and glutamine-utilizing site location. Biochemistry 26:1940–1948

Born M (1920) Volumen und Hydrationswärme der Ionen. Z Phys 1:45–48

Chmara H, Andruszkiewicz R, Borowski E (1985) Inactivation of glucosamine 6-phosphate synthetase from *Salmonella triphimurium* LT2 by fumaroyl diaminopropionic acid derivatives, a novel group of glutamine analogs. Biochim Biophys Acta 870:357–366

Clowell SM, Marshall AR, Amos RD, Handy NC (1985) Quantum chemistry on microcomputers. Chem Br 21:655–659

Dewar MHS, Thiel W (1977) Ground states of molecules XII: Development of the new MNDO method. J Am Chem Soc 99:4899–4907

Dijkman JP, Osman R, Weinstein H (1987) Practical considerations in calculations of the proton transfer in a model active site of papain. Int J Quant Chem: Quant Biol Symp 14:211–219

Drenth J, Kalk KH, Swen HM (1976) Binding of chloromethyl ketone substrate analogs to crystalline papain. Biochemistry 15:3731–3738

Lewis SD, Johnson FW, Shafer J (1976) Potentiometric determination of ionization at the active site of papain. Biochemistry 15:5009–5017

Liwo A, Tempczyk A, Grzonka Z (1988) Molecular mechanics calculations on deaminooxytocin and deamino-arginine-vasopressin and its analogues. J Comput-Aided Mol Design 2:271–309

Liwo A, Tempczyk A, Grzonka Z (1989) Theoretical studies of the mechanism of the action of the neurohypophyseal hormones. Part I: Molecular electrostatic potential and molecular electrostatic field maps of some vasopressin analogues. J Comput-Aided Mol Design 3:261–284

Milewski S, Chmara YH, Andruszkiewicz R, Borowski E, Zaremba M, Borowski J (1988) Antifungal peptides with novel specific inhibitors of glucosamine-6-phosphate synthase. Drugs Exp Clin Res 14:461–465

Polgar L (1974) Mercaptide-imidazolium ion pair. Reactive nucleophile in papain catalysis. FEBS Lett 47:15–18

Shinitzky R, Goldman R (1967) Fluorometric detection of histidine-tryptofan complexes in peptides and proteins. Eur J Biochem 3:139–144

Tempczyk A, Tarnowska M, Liwo A (1989) A theoretical study of glucosamine synthase. Part I: Molecular mechanics calculations on substrate binding. Eur Biophys J 17:201–210

Umeyama H, Nagakawa S (1981) Molecular orbital study of proton transfer energetics in the active site of papain by using methanethiol-imidazoleformic acid complex as a model. Chem Pharm Bull 29:918–925

Weiner SJ, Kollman PA, Case, DA, Singh UC, Ghio C, Alagona G, Profeta S, Weiner P (1984) A new force field for molecular simulation of nucleic acids and proteins. J Am Chem Soc 106:765–784